

# Pile to Slab Bridge Connections

Mohamed I. Ayoub<sup>1</sup>, David H. Sanders<sup>2</sup> and Ahmed Ibrahim<sup>3</sup>

## Abstract

Slab bridges are a common bridge type, where the pile extends directly from the ground to the superstructure. Most codes provide little direct design guidance for pile extension connection details for slab bridges. Unlike the column to box-girder bridge connections, which are often under extensive discussion, slab-bridge connections are rarely discussed. The project results will provide standardized details as well as rational methodology for designing and analyzing these connections. Eight large to full-scale column-slab bridge connection will be tested in this study. Column (pile)-slab connections include drop cap-column, flat slab-column, and knee. The first two columns have been tested and two others specimens are preparing for testing. The paper will discuss model selection and design, test setup, instrumentation of the specimens, loading program, observation during tests and the future steps.

## Introduction

The State of California has a large number of highway bridges; many of them are slab bridges. Although slab bridges are a common type of bridge, the current version of the Bridge Design Specification (BDS) [Caltrans, 2006] and the Seismic Design Criteria (SDC) [Caltrans, 2007] provides little direct design guidance for pile extension connection details for slab bridges. The drawings for slab bridges examined in this study are extracted from the Bridge Design Aid (BDA) [Caltrans, 2004] of Caltrans. This project focuses on the design and detailing of the connection region for pile extension to slab bridges, see Figure 1.

In the analytical study, the XTRACT program [Imbsen, 2006] is used to predict the moment curvature for the cross sections. Non-linear SAP2000 [Computer and Structures, 2008] and Opensees [2008] are run on sample bridges to determine the moment inflection points in the columns and the overall behavior of the system. Strut-and-tie models, as well as simplified procedures, will be developed for the joint region. The paper will discuss the experimental results to date.

## Model Section and Design

The embedded length of the column varies according to the soil type. In the plans submitted by Caltrans to University of Nevada, Reno (UNR), the height of the column above the ground ranged from 9D to 20D. Therefore, an average height of the column above the soil surface equals 14.5D. The point of the maximum moment for the individual column can be approximated at D to 2D under the surface of the soil as shown in Figure 2. This increases the average total length to 15.5D to 16.5D, the column inflection point was chosen to be approximately halfway between column top and maximum moment point in the soil. Therefore, the data indicates that the columns are typically flexural members. Columns with shear lengths

<sup>1</sup> Graduate Research Assistant, Dept. of Civil and Environmental Engineering, University of Nevada, Reno

<sup>2</sup> Professor, Dept. of Civil and Environmental Engineering, University of Nevada, Reno

<sup>3</sup> Senior Bridge Engineer, California Department of Transportation, Sacramento, CA

equal or greater than 6D are considered flexural members. Therefore, the height of the specimen was chosen to be 7D. The effective slab length of the specimen in the direction of loading (transverse of the bridge) is determined by the distance between the points of zero moment due to lateral load as shown in Figure 3.

**Test Setup:** The test setup was selected to provide the same loading as the actual bridge. A comparison between Figures 3 and 4a shows the same moments at the joint. The transfer of axial loads to the specimen was accomplished through a steel I-beam that was placed across the column top as shown in Figure 4b. The initial axial load force was applied by means of hydraulic jack on top of the I-beam. Prestressing bars were extended vertically and anchored at the top of the jacks and the bottom of the slab. Longitudinal beams were used beneath the slab to transfer the force to the slab. To minimize axial load fluctuation under different drift levels, a pressure accumulator was hooked to the hydraulic system between the pump and the jacks. At the beginning of each test, the desired axial load was applied prior to lateral loading. To create the inflection point and prevent moment generation at the slab ends, hinges were used to enable the slab to rotate (see Figure 4b). Lateral load was applied by means of a 220-Kip MTS hydraulic actuator. The actuator was connected to reaction blocks. In its initial position, the actuator was level and had a potential maximum stroke of plus/minus 15 inches (380 mm)

**Basic Specimen Configuration:** To determine the effective width of the specimen in the longitudinal direction of the bridge, T-beam models were used according to Section 8.10.2 of ACI 318-05 [American Concrete Institute, 2005], the connection dimensions represent the effective slab width. The effective width of a T-beam flange should not exceed the following Eqs. 1 to 5.

One-quarter of the span length of the beam (Eq. 1)

Web width + eight times the slab thickness on each side (Eq. 2)

Web width + 1/2 the clear distance to the next web on each side (Eq. 3)

The effective width as T-beam flange should be bigger or equal to the following Equations (Eq. 4) and (Eq. 5).

The effective width  $(b_e) \geq 2$  the width of the beam  $(bb)$  (Eq. 4)

The effective width  $(b_e) \geq (2h+2h+D)$  (Eq. 5)

Where:

$(h)$  = the beam depth,  $(D)$  = the diameter of the column and  $(b_e)$  = the effective width of the slab.

**DCRCCI Reinforcement:** This specimen represents the slab-column connection for a 34-ft (10.4-m) multi-span bridge. The reinforcement is the same as what would be found in the prototype bridge since the specimen is full scale (see Figure 5)

**FSRCCI Reinforcement:** This specimen represents the slab-column connection for a 24-ft (7.3-m) two-span bridge. The reinforcement is the same as what would be found in the prototype bridge since the specimen is full scale (see Figure 6).

## **Instrumentation**

The specimens were instrumented with an array of strain gauges, linear variable differential transformers (LVDT's), and load cells. Longitudinal and transverse reinforcement in the column and slab region were instrumented with strain gauges. Strain in the concrete and curvature along the potential plastic hinge length of the column were determined by means of five pairs of LVDT's. The LVDT's were placed within a height of 20 inches (500 mm) from the bottom of the column as shown in Figure 7. The lateral deflection of the column was measured along the center-line of the lateral load. Vertical and lateral loads were monitored by load cells.

## **Loading Program**

The basic test program will be the same for all eight specimens. The axial load will depend on the particular case. The cyclic loading (see Figure 8) is divided into two parts: force control and displacement control. The load is increased until it reaches 75 % of the estimated yield load. A displacement ductility of one is based on the displacement of 4/3 times the displacement at 75% of the estimated yield load. The specimen was considered to be failed when the lateral load capacity for the specimens dropped to 80% of its maximum capacity.

## **Observed Response**

***Specimen DCRCC1:*** The specimen was subjected to constant axial load equal to 76.40 kips (340 kN). This is approximately  $0.072f'_c A_g$  of the column. Due to the column deflection, the axial load generates a horizontal component in the opposite direction of the horizontal force of the actuator, so the horizontal force must be corrected. The corrected force-displacement relationship for the experimental results (Push-over curve) is plotted as shown in Figure 9. The hysteretic load-displacement response of specimen DCRCC1 is shown in Figure 10. At displacement ductility ( $\mu_\Delta$ ) of approximately  $\pm 1$ , the specimen did not show signs of strength decay or significant stiffness degradation. During the second excursion of  $\mu_\Delta = \pm 2$ , slight stiffness degradation was apparent. When the specimen was taken to the second cycle of  $\mu_\Delta = \pm 2$ , the concrete started to spall on both sides of the column. The peak measured lateral load was 15.1 kips (67.2 kN). The peak load occurred at the end of the second excursion of  $\mu_\Delta = \pm 2$ . As the specimen was pushed to higher ductility, the cover concrete at the bottom of the column spalled off at an increasing rate. Flexural cracks also developed along the column height. During the first excursion of  $\mu_\Delta = \pm 4$  the cracks started to widen and the spiral and longitudinal reinforcement started to be exposed. When the specimen was pushed to 14.15 in (359 mm), the longitudinal bars on the compression side were completely buckled and the spiral fractured.

At a load equal to 75% of the maximum load, the displacement was equal to 1.768 in (44.9 mm) and ductility displacement was set at  $0.75\mu$ . Therefore at the ultimate displacement of 14.15 in (359 mm), produces a ductility of  $\mu_\Delta = 5.98$ . Figure 11 shows the specimen during last stages of the test. At the end of the test the slab had no significant crack and all the failure occurred in the

column. A review of the strain gauge data revealed that the yielding occurred in the longitudinal and transverse reinforcement of column. The yielding occurred in the longitudinal column reinforcement at an early stage of the test before reaching the calculated effective section yield. Some of the transverse reinforcement in the column and in the connection yielded towards the end of the test. Longitudinal slab reinforcement did yield, and slab stirrups showed high strains.

**Specimen FSRCC:** The specimen was subjected to constant axial load equal to 70.40k (313.2 kN). This is approximately  $0.078f'c A_g$  of the column. The corrected force-displacement relationship for the experimental results (Push-over curve) is plotted in Figure 9. The hysteretic load-displacement response of specimen FSRCC1 is shown in Figure 12. At displacement ductility ( $\mu_{\Delta}$ ) of approximately  $\pm 1$ , the specimen did not show signs of strength decay or significant stiffness degradation. During the second excursion of  $\mu_{\Delta} = \pm 2$ , slight stiffness degradation was apparent. When the specimen was taken to the second cycle of  $\mu_{\Delta} = \pm 2$ , the concrete started to spall on both sides of the column. The peak measured lateral load was 15.15 kips (67.39 kN) The peak load occurred at the end of the second excursion of  $\mu_{\Delta} = \pm 3$ . As the specimen was pushed to higher ductility, the cover concrete at the bottom of the column spalled off at an increasing rate. Flexural cracks also developed along the column height. During the second excursion of  $\mu_{\Delta} = \pm 4$  one of the longitudinal bars fractured. During the first excursion of  $\mu_{\Delta} = \pm 5$  the spiral and longitudinal reinforcement were exposed. Spalling appeared on the slab as shown in Figure 13. When the specimen was pushed to 14.34 inches (364 mm), the longitudinal bars on the compression side completely buckled and the spiral fractured. The ultimate displacement was 12 in at a  $\mu_{\Delta}$  of 5.80 and a load of 12.12 kips (53.91 kN) (80% of the maximum load). Figure 14 shows the specimen during last stages of the test. A review of the strain gauge data showed that yielding occurred in the column longitudinal reinforcement. One column transverse reinforcement strain gauge showed yielding towards the end of the test. The column transverse reinforcement in the connection had high strains but did not yield. None of the slab longitudinal reinforcement yielded. The slab transverse stirrups showed high strains, but didn't yield.

### **Future Steps**

Two specimens will be tested soon at the University of Nevada, Reno. The pile diameters have been increased to 24 in. Since that there are no equations to check the shear reinforcement in the slab, the equations of the box-girder were used. One specimen was designed with a drop-cap and the other one with a flat-slab. A knee-joint connection is also very critical (see Figure 1). It is likely that this type of connection will also be tested. In this case, variable axial load will be used since overturning can cause changes in axial load.

### **Conclusions**

- 1-A review of the strain gauges data revealed that the yielding occurred in the longitudinal and transverse steel of column. The longitudinal development length inside the slab is sufficient.
- 2- Confinement detailing was sufficient to permit the specimens to reach a ductility level of 6.
- 3- After finishing the tests, the slabs were checked to see if there were any cracks from the bottom and top.

The visual inspection showed that there were no cracks in DCRCC1. Minor cracks were seen

because of surface spalling as mentioned before in FSCRCC1. That inspection proved that the design of slab was good.

4-The data of the LVDT's on the sides of the slab didn't record any significant shear displacement.

5-Current Caltrans details provide conservative slab designs and promote plastic hinging in the columns.

### **Acknowledgements**

This studying was funded by the California Department of Transportation (CALTRANS), under contract 04-EQ092. Their support and expertise is critical to this project and is greatly appreciated. However the findings and the conclusions by the authors do not necessarily represent the views of CALTRANS.

### **References**

ACI Committee 318, "Building Code Requirements for Reinforced Concrete (ACI 318-05) and Commentary (318M-05)," American Concrete Institute, Farmington Hills, Mich., ACI 318M-05, 101 pp.

Caltrans (2007) "Bridge Design Specification", Caltrans, Sacramento, CA August (2007).

Caltrans (2006) "The Seismic Design Criteria" Version 1.4, Caltrans, Sacramento, CA June (2006).

Caltrans (2004) "Standard Slab Bridge-General Instructions," Bridge Design Aides 4-104. Caltrans, Sacramento, CA September (2004).

Computer and Structures, Inc (2008), Sap2000 Software, Computer and Structures, Inc.

Imbsen Software Systems (2008), XTRACT Software, [www.imbsen.com](http://www.imbsen.com)

Opensees (2008), Pacific Earthquake Engineering Research Center, University of California, Berkeley, <http://opensees.berkeley.edu>.

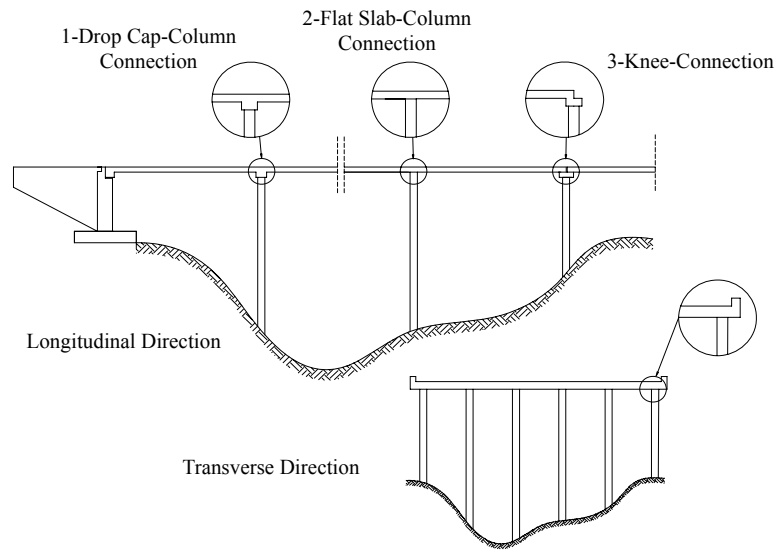


Figure. 1 Slab Bride Connections.

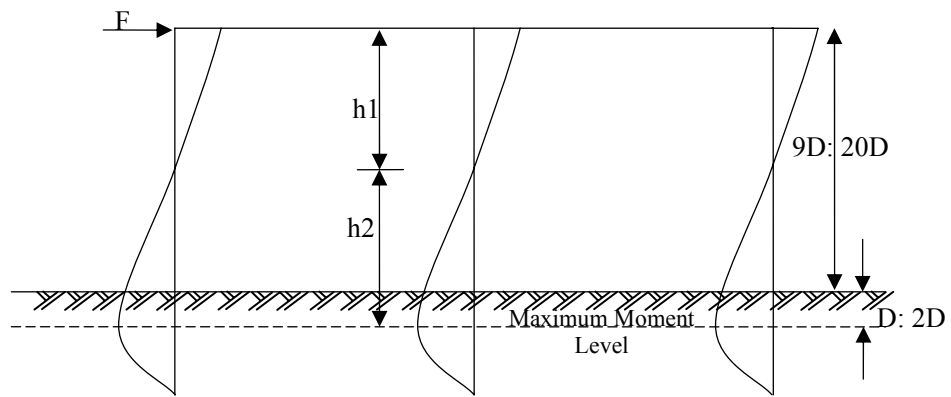


Figure 2 Typical Moment Diagram for Lateral

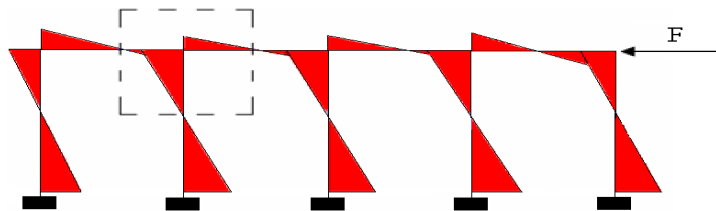


Figure 3 Moment Diagram System for Lateral Load

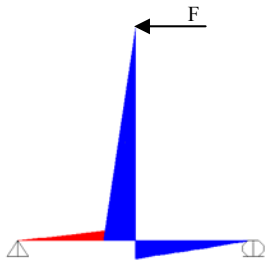


Figure 4a Moment Diagram from Test Setup

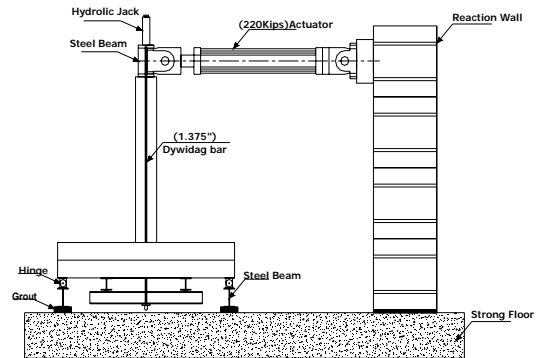


Figure 4b Test Setup

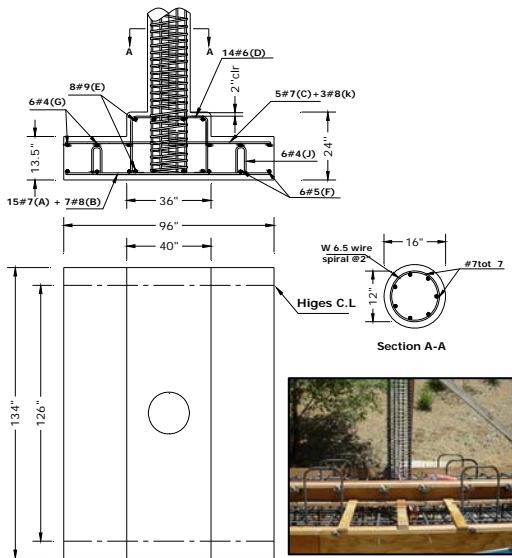


Figure 5 DCRC1 Specimen Dimensions and Reinforcement

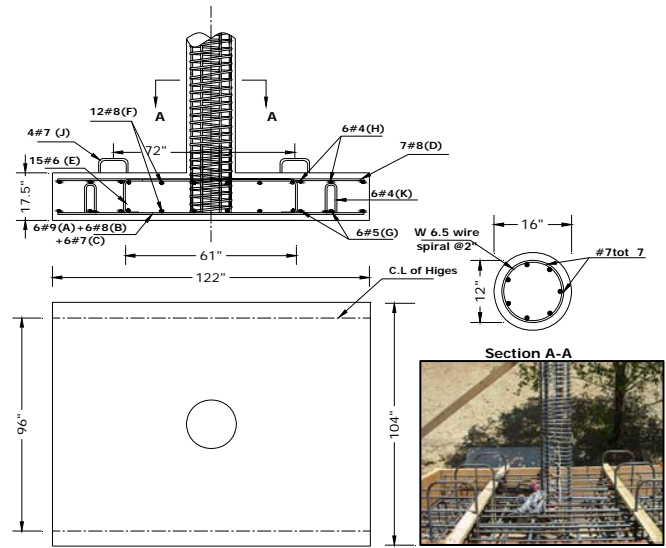


Figure 6 SRCC1 Specimen Dimensions and Reinforcement

1" = 25.4 mm

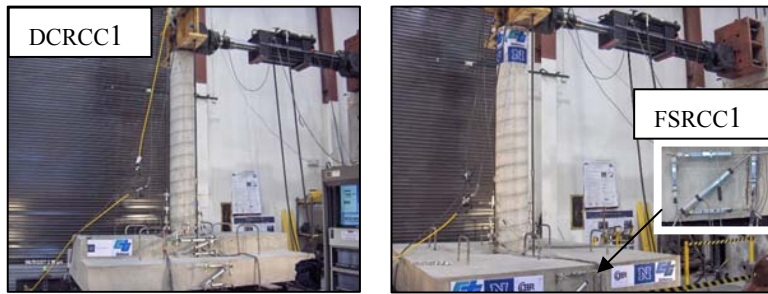


Figure 7 LVDT's Instruments

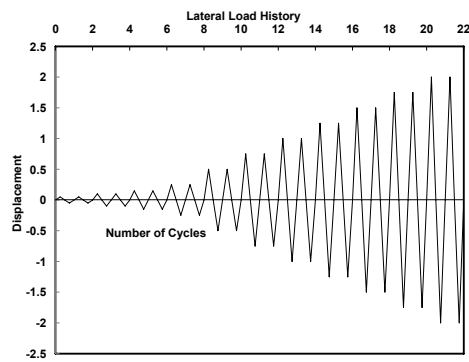


Figure 8 Typical Cyclic Load Diagram

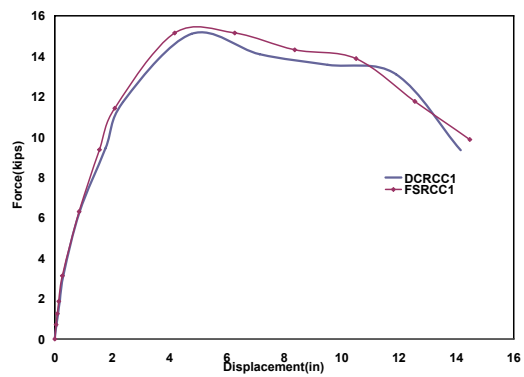


Figure 9 Push-Over Curve

1 " = 25.4 mm and 1 kip = 4.45 kN

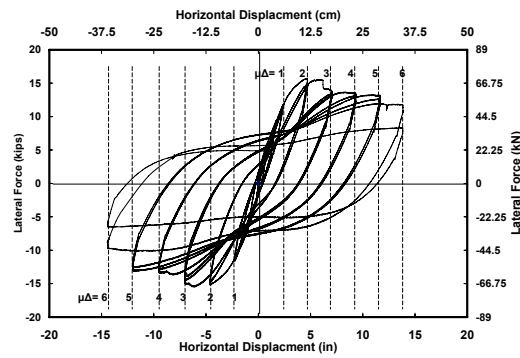


Figure 10 Measured Lateral Load-Deflection Hysteresis Loops - DCRCC1

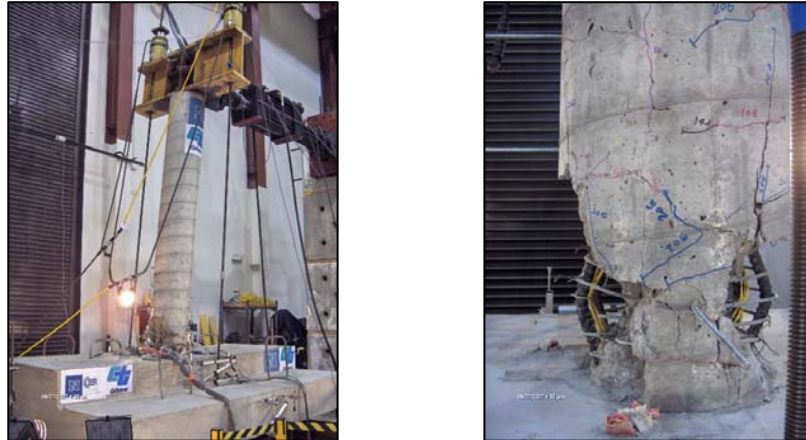


Figure 11 Specimen DCRCC1 During Last Stage

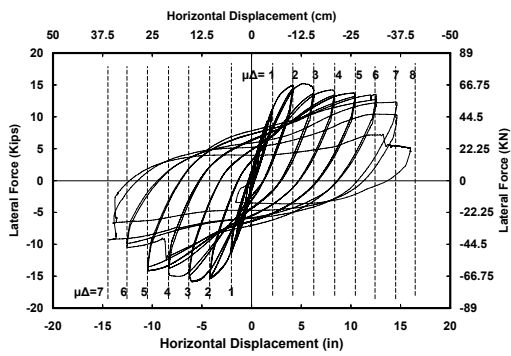


Figure 12 Measured Lateral Load-Deflection Hysteresis Loops - FSRCC1



Figure 13 Minor Cracks on the Slab Surface



Figure 14 Specimen FSRCC1 During Last Stage